frontiers in Astronomy and Space Sciences

DATA REPORT
published: 07 May 2021
doi: 10.3389/fspas.2021.662545

The Vertical and Adiabatic Ionization Energies of Silicon Carbide Clusters, $(SiC)_n$, With n = 1–12

*David Gobrecht**

Department of Physics and Astronomy, Institute of Astronomy, KU Leuven, Leuven, Belgium

Keywords: silicon carbide, ionization, clusters, cations, nucleation, dust formation, circumstellar

Edited by:
Ryan C. Fortenberry,
University of Mississippi, United States

Reviewed by:
Helgi Rafn Hrodmarsson,
Leiden University, Netherlands
Marzio Rosi,
University of Perugia, Italy

****Correspondence:***
David Gobrecht
dave@gobrecht.ch

Specialty section:
This article was submitted to Astrochemistry, a section of the journal Frontiers in Astronomy and Space Sciences

Received: *01 February 2021*
Accepted: *06 April 2021*
Published: *07 May 2021*

Citation:
Gobrecht D (2021) The Vertical and Adiabatic Ionization Energies of Silicon Carbide Clusters, $(SiC)_n$, With n = 1–12. Front. Astron. Space Sci. 8:662545. doi: 10.3389/fspas.2021.662545

1. INTRODUCTION

The chemistry occurring in astrophysical environments is primarily controlled by the carbon-over-oxygen (C/O) ratio. This is a consequence of the high carbon monoxide (CO) bond energy of 11.2 eV making CO the most stable diatomic molecule known (Luo, 2007). This classical dichotomy is challenged since non-equilibrium processes such as photo-chemistry and pulsation-induced shocks can break the strong CO bond and lead to the formation of unexpected molecules (Agúndez et al., 2010; Gobrecht et al., 2016). Of particular astronomical interest are refractory molecules and molecular clusters that represent the precursors of circumstellar dust. One of the main dust species in carbon-dominated regimes is silicon carbide (SiC). A broad spectral feature around 11.3 micron is commonly observed in Carbon-rich evolved starts and attributed to the presence of SiC dust grains (Friedemann, 1968; Hackwell, 1972; Treffers and Cohen, 1974). SiC stardust was extracted from pristine meteorites (Bernatowicz et al., 1987; Amari et al., 1994; Hoppe et al., 1996; Zinner et al., 2007; Liu et al., 2014). Recent studies have shown that the vast majority of presolar SiC grains found in pristine meteoritic stardust originate from low-mass Asymptotic Giant Branch (AGB) stars (Cristallo et al., 2020). But also molecular gas-phase species like SiC, Si_2C, SiC_2 were detected in the circumstellar envelopes of carbon-rich evolved stars (Thaddeus et al., 1984; Cernicharo et al., 1989; McCarthy et al., 2015; Massalkhi et al., 2018). The evidence for both, gas-phase silicon-carbon molecules and solid SiC dust suggests that their intermediaries, i.e., SiC molecular clusters, also exist in carbon-rich astronomical environments and partake in the nucleation and SiC dust formation process.

Therefore, SiC molecular clusters are the objects of our interest. This study represents a continuation of a prior work (Gobrecht et al., 2017) and addresses the (single) ionization energies of the previously investigated neutral $(SiC)_n$, n = 1–12, clusters. This paper is organized as follows. In section 2, we present the methods used to derive the vertical and adiabatic ionization energies. Section 3 shows the results for these energies as well as the adiabatically optimized cation geometries and in section 4 our summary and conclusion is given.

2. METHODS

In this study, we focus on small, singly ionized silicon carbide cation clusters with a silicon-to-carbon stoichiometry of 1:1, $(SiC)_n{}^+$. The smallest lowest-energy neutral $(SiC)_n$, $n = 1-11$, clusters are characterized by atomic segregation of carbon and silicon (Hou and Song, 2008; Duan et al., 2013; Byrd et al., 2016). The carbon atoms tend to form chains and benzene-like rings, whereas the silicon atoms develop triangular and tetrahedral substructures bridging to the carbon segregation. The presence of aromatic carbon rings in the neutral $(SiC)_n$ Global Minima (GM) candidates indicates the occurrence of strongly bound, delocalized valence electrons.

We investigate the vertical and adiabatic single-electron ionization energies of (SiC)$_n$, n = 1−12, clusters by means of Density Functional Theory (DFT). The energies and geometries of the lowest-energy neutral isomers (i.e., GM candidates) were already presented in a previous study (Gobrecht et al., 2017). These calculations were performed on the M11/cc-pVTZ level of theory (Peverati and Truhlar, 2012), which was shown to result in accurate energies with affordable computational cost and, in contrast to the B3LYP functional, is not outperforming (Byrd et al., 2016). For consistency and comparability, the (SiC)$_n^+$ cluster calculations were also performed on the same level of theory (M11/cc-pVTZ). For the DFT calculations we use the computational software Gaussian 09 (Frisch et al., 2009). For all optimizations a vibrational frequency analysis is performed. First, it allows us to discriminate between Transition States (TSs) exhibiting one imaginary frequency and true minima with only real vibration modes. In the case of a TS, marking a saddle point on the potential energy surface, the geometry is distorted in direction of the negative curvature of the saddle point and re-optimized to obtain a real minimum. Second, partition functions can be constructed to calculate thermodynamic potentials within the Rigid Rotor Harmonic Oscillator (RRHO) appromixation. Third, the resulting vibrational spectra can be compared with observational data.

The current work represents an extension of a previous (SiC)$_n$ cluster study (Gobrecht et al., 2017), which did not comprise the ionization of these clusters and its related cations. Owing to the enormous computational task, we did not perform global optimization searches of the (SiC)$_n^+$ cations themselves. Instead, we perform ionization calculations for the four lowest-lying neutral isomers for each size *n*. As mentioned in (Gobrecht et al., 2017), the GM candidate isomer may not be the most favorable structure in circumstellar conditions and hence it is required to study a range of the energetically lowest-lying structures and their respective cations for each cluster size. Therefore, we assume that the neutral (SiC)$_n$ clusters are initially present in the form of their four lowest-energy isomers including their GM candidate structure, and that they are subsequently ionized. We are aware that our set of isomers is not complete and hence, there is the possibility that (SiC)$_n$ cation isomers with a lower energy exist. In order to reduce this possibility and to avoid missing a particularly stable SiC cluster cation, additional test calculations for different geometries (e.g., cages and tubes) are performed.

It is known that neutral molecules and related clusters can alter their ground-state geometry significantly upon the loss of an electron. They include, for example, clusters of water (Belau et al., 2007) and Argon (Briant et al., 2012), but also organic compounds like methyl ketene (Derbali et al., 2020), acetic acid (Guan et al., 2012), or δ-Valerolactam (Mahjoub et al., 2011). Moreover, the spin-degenerate cluster cations can be subject to Jahn-Teller effects implying a lowering of their spatial symmetry and a structural rearrangement. Therefore, it is instructive to not only study the *vertical* ionization energies, corresponding to single point energy evaluations, but also *adiabatic* ionization energies taking into account structural rearrangements. Here, all cations are presumed to be in a doublet state (i.e., with a spin multiplicity of 2), since the neutral (SiC)$_n$, $n \geq 2$, clusters are singlet states and the SiC molecule (n = 1) is in a triplet state.

TABLE 1 | Vertical and adiabatic ionization energies, E_n^{vert} and E_n^{adia}(in eV), and their difference $\Delta E = E_n^{vert}-E_n^{adia}$, of (SiC)$_n$ clusters vs. cluster size *n*.

n	E_n^{vert}	E_n^{adia}	ΔE
1	10.64	10.64	0.00
2 *LM*	10.01	9.87	0.14
2 *GM*	8.27	8.21	0.07
3 *TS*	9.34	8.95	0.39
3 *LM*	9.34	8.77	0.57
3 *GM*	8.17	7.94	0.22
4 *TS*	8.78	8.63	0.15
4 *LM*	8.78	8.23	0.55
4 *GM*	7.62	7.36	0.27
5 *TS*	7.94	7.75	0.18
5 *GM*	7.94	7.61	0.33
6	7.90	7.46	0.44
7	7.56	7.25	0.31
8	7.22	6.85	0.37
9	7.34	6.96	0.38
10	7.20	6.95	0.25
11	6.82	6.64	0.18
12	6.69	6.59	0.10

LM corresponds to a Local Minimum cation geometry, GM to a Global Minimum cation geometry, and TS to a Transition State, respectively.

3. RESULTS

In the following, we present the vertical and adiabatic ionization energies of (SiC)$_n$, n = 1−12, clusters and the related structures of the adiabatically optimized, singly ionized (SiC)$_n^+$, n = 1−12, cations.

3.1. Vertical Ionization

The vertical ionization energies, E_n^{vert}, are listed in **Table 1**. E_n^{vert} of the lowest-energy cations (denoted with GM) show an overall monotonically decreasing trend with cluster size *n*, starting from 10.64 eV (n = 1) to 6.69 eV (n = 12), with opposing tendencies at n = 5 and n = 9. For the smallest sizes (n = 1−2) E_n^{vert} decrease more strongly than for larger sizes. For the latter size regime the decrease in E_n^{vert} flattens, except for n = 9, where E_9^{vert} = 7.34 is slightly larger than for n = 8 and n = 10. Considering only structural analogs of the neutral GM clusters (denoted as LM), we find a similar decreasing trend with cluster size *n*, except for n = 9.

3.2. Adiabatic Ionization

In this subsection, we discuss the adiabatic ionization energies E_n^{adia} and compare their respective geometries with those of the neutral clusters. In **Figure 1**, the lowest-energy cation structures are shown. Cation isomers that are derived from neutral GM candidates (i.e., structural twins or analogs), but which are metastable with respect to the lowest-energy cations, are depicted

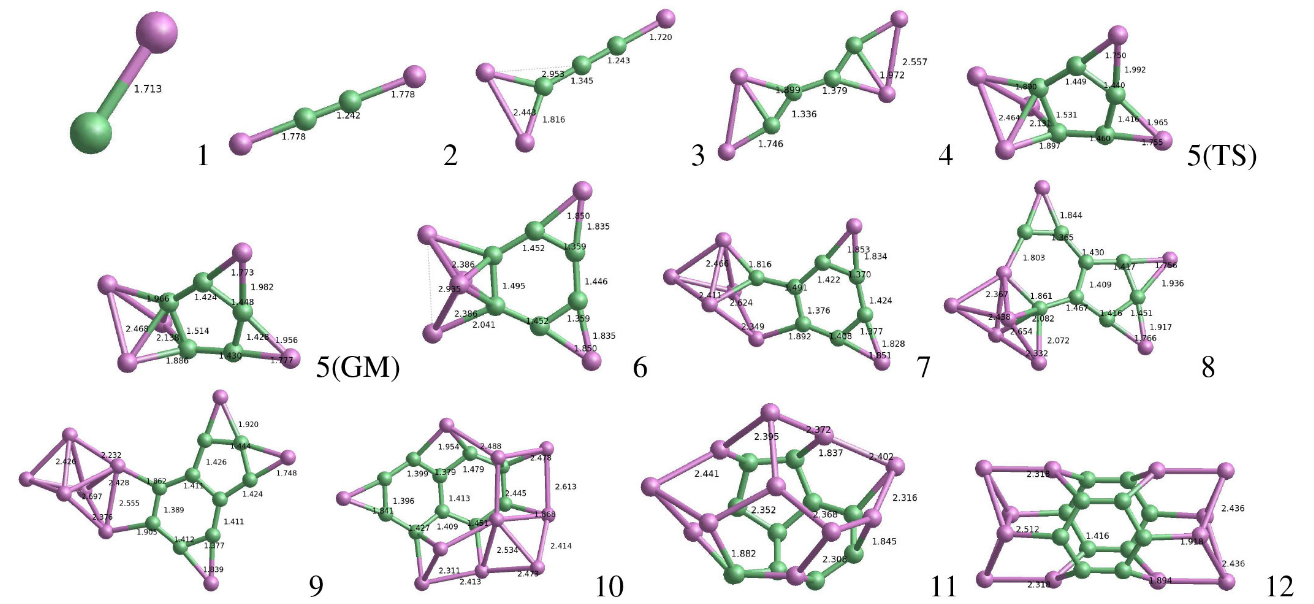

FIGURE 1 | Electronic structures of the lowest-energy $(SiC)_n{}^+$, n = 1−12, cations. Silicon atoms are displayed in purple, carbon atoms in green. Bond lengths and distances are given in Å. The cluster size *n* is given at the right bottom of the corresponding structure.

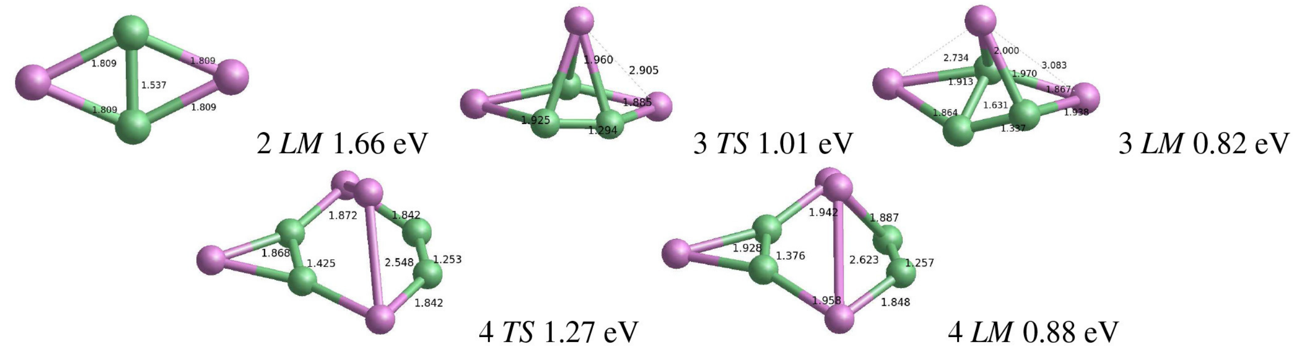

FIGURE 2 | Electronic structures of metastable $(SiC)_n{}^+$, n = 2–4, cations corresponding to the structural analogs of the neutral Global Minima (GM) clusters. Silicon atoms are displayed in purple, carbon atoms in green. Bond lengths and distances are given in Å. The cluster size *n*, the type (*LM*, Local Minimum; *TS*, Transition State) and the relative energy is given at the right bottom of the corresponding structure.

in **Figure 2**. For comparison we also display the neutral GM candidates in **Figure 3** and local minima neutral isomers (see **Figure 4**) corresponding to the structural analogs of the lowest-energy cations.

The triplet ground state of the neutral SiC molecule has a bond length of 1.707 Å (see **Figure 1**). The adiabatically optimized SiC^+ cation is assumed to be a doublet state and has a slightly larger bond length of 1.713 Å. The energy difference of vertical and adiabatic ionization is negligible (0.002 eV). In comparison to the experimentally derived ionization energy of 9.2 eV (Drowart et al., 1958) and to the value of 8.7 ± 0.2 from a previous theoretical investigation (Boldyrev et al., 1994), we obtain a higher value (10.64 eV) for the SiC ionization potential.

For the SiC dimer, $(SiC)_2$, a linear Si-C-C-Si geometry represents the lowest-energy cation structure (see **Figure 1**), which is different from the diamond shaped neutral GM candidate shown in **Figure 3**. In comparison with the linear geometry of the neutral dimer (see **Figure 4**), the two Si-C bonds in the cation are larger by 0.055 Å and the C-C bond increases by 0.031 Å. The adiabatic ionization energy is 7.81 eV with respect to the neutral GM candidate and 7.52 eV with respect to the neutral Si-C-C-Si chain. The rhombic (diamond-shaped) $(SiC)_2$ cation shown in **Figure 2**, resembling the neutral GM candidate, lies 9.87 eV above the latter. In this cation, the C-C bond distance is increased from 1.421 to 1.537 Å and the four Si-C bonds are decreased from 1.827 to 1.809 Å, when adiabatically ionized.

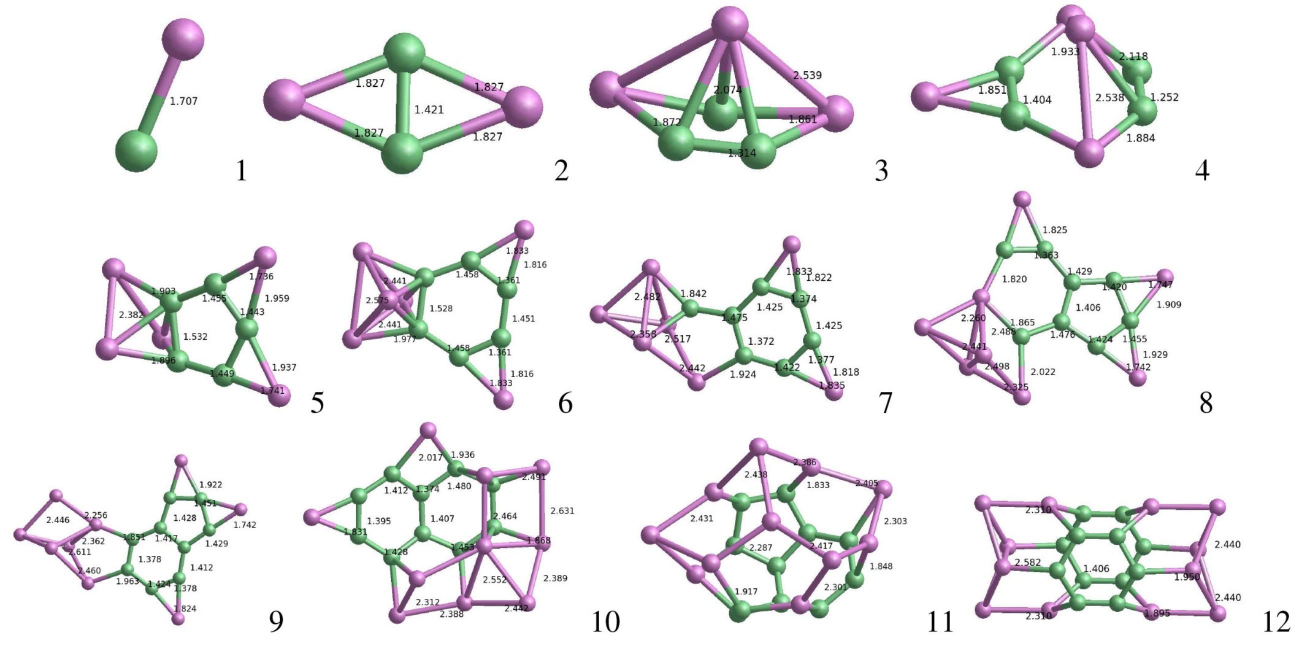

FIGURE 3 | Electronic structures of neutral (SiC)$_n$, n = 1−12, global minima (GM) candidates. Silicon atoms are displayed in purple, carbon atoms in green. Bond lengths (in Å) are indicated by numbers. The cluster size *n* is given at the right bottom of the corresponding GM structure.

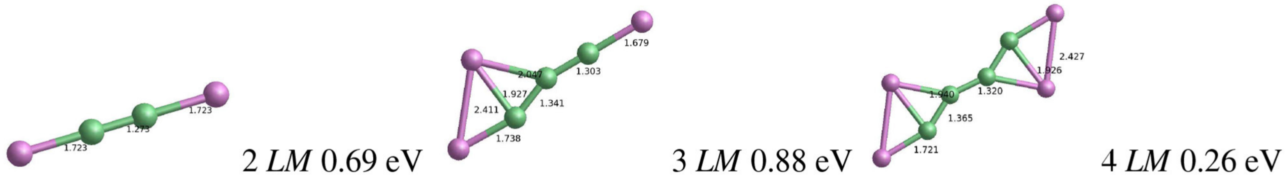

FIGURE 4 | Electronic structures of neutral (SiC)$_n$, n = 2−4, local minima candidates (denoted as *LM*) corresponding to the structural analog of the most favorable (SiC)$_n$$^+$, n = 2−4, cations. The cluster size *n* at the relative energy is given at the right bottom of the corresponding structure.

This indicates that a double bonded C=C in the neutral (SiC)$_n$ becomes single bonded in the related cation.

Other isomers show ionization energies in the range of 8.48−14.05 eV. For n = 3, the lowest-energy cation in our set corresponds to a structurally different isomer than the neutral GM (see **Figures 1**, **3**). It has an energy of 7.94 eV above the neutral GM and 7.04 eV above its neutral structural twin. The largest geometric change upon the loss of an electron consists in the breaking of a bond (marked with dashed line and labeled with a distance of 2.953 Å in **Figure 1**), which is present in the neutral isomer (2.047 Å). The other bond lengths change by 0.03−0.11 Å. The cationic twin of the neutral GM displayed in **Figure 2** has an energy 1.01 eV above the lowest-energy cation and is a TS, whose distorted, asymmetric geometry results in a real minimum with a relative energy of 0.88 eV. These cations show increased Si-Si distances as compared with the neutral GM. Further investigated trimer isomers have ionization energies in the range of 8.20−10.26 eV.

The adiabatic ionization of different (SiC)$_4$ isomers shows that the lowest-energy cation is a structural analog of the second most favorable neutral structure (see **Figures 1**, **4**). The GM cation has an adiabatic ionization energy of 7.36 eV with respect to the neutral GM and 7.07 eV with respect to the neutral structure analog. It consists of a C$_4$ chain in a trans configuration with two Si atoms arranged at each of the two tails of the chain. Upon the loss of an electron, most significantly, the two Si-Si bonds increase by 0.13 Å among minor changes in the other bond lengths. As for n = 3, the optimized (SiC)$_4$$^+$ structural twin of the neutral GM shows an imaginary vibrational frequency and is a TS with an energy of 8.63 eV above the neutral GM. To obtain a real minimum, a further optimization is performed leading to a symmetry breaking of the C$_2$-Si-C$_2$-Si ring structure by increasing two Si-C bond lengths and by tilting the quasi planar ring structure. The local minimum lies about 0.40 eV below the TS. Other cation isomers show ionization energies of 7.41−7.84 eV.

The most favorable $(SiC)_5{}^+$ cation resembles its neutral analog and has an ionization energy of 7.61 eV. However, in contrast to its neutral counterpart the two out-of-plane Si atoms increase their distance to each other by 0.25 Å. This structure is a TS and a subsequent optimization to a real minimum leads (as for n = 3 and 4) to a breaking of the C_{2v} symmetry. In the real minimum cation, the two out-of-plane Si atoms have distance of 2.63 Å to each other (like in the neutral cluster), but are shifted into the display plane, which reduces the energy by 0.14 eV (as compared to the TS). The ionization energies of other investigated isomers range from 7.90 to 8.32 eV.

For n = 6, the lowest-energy cation is a structural analog of the neutral GM candidate with an ionization energy of 7.46 eV. Its overall geometry hardly changes by the adiabatic ionization. The C-C and Si-C bond distances are largely preserved. The biggest change occurs at two Si atoms increasing their distance by 0.30 Å. This likely to be the place, where the loss of the electron occurred during the adiabatic ionization, which accounts for 0.44 eV. We find ionization energies of 7.50−8.45 eV for other hexamer cation isomers.

The lowest-energy $(SiC)_7{}^+$ cation resembles the neutral $(SiC)_7$ GM cluster and lies 7.25 eV above it. The largest changes in the bond distances occur at Si-Si bonds that lie out-of-plane. The difference in the vertical and adiabatic ionization energy (0.31 eV) is smaller than for n = 6 and n = 8. Further $(SiC)_7{}^+$ isomers exhibit ionization energies of 7.60−8.26 eV.

For n = 8, an ionization energy of 7.25 eV is found for the lowest-energy cation, which is a look-alike of the neutral GM candidate. The largest atomic mobility during the adiabatic ionization is accomplished by the out-of-plane Si atoms. These two Si atoms have moved closer to the C atom and are now four-fold coordinated, in comparison to the neutral $(SiC)_8$ cluster, where these Si atoms are three-fold coordinated. The adiabatic structure change results in a lower energy of 0.37 eV. For other isomers we find ionization energies of 7.62−7.73 eV.

For n = 9, the neutral GM and lowest-energy cation exhibit a similar shape and differ by 6.96 eV in energy. Its adiabatic ionization affects predominantly the silicon-segregated part of the isomer. The two Si atoms out-of-plane increase their distance to each other, whereas two Si atoms in the plane move closer to each other accounting for 0.38 eV. Other local minima have ionization energies of 7.11−7.64 eV.

For n = 10, both the neutral $(SiC)_{10}$ clusters and its cation $(SiC)_{10}{}^+$, do not exhibit planar carbon ring structures, but are strained. This is the smallest cluster/cation size, where the C atoms do not lie in a planar configuration. The lowest-energy $(SiC)_9{}^+$ cation geometry corresponds to the one of the neutral GM candidate and has a relative energy of 6.95 eV. The largest impact on the geometry is found to be located at a single Si atom. In the cation this Si atom is connected to the silicon subcluster, whereas in the neutral cluster it binds only to C atoms. This Si migration causes an energy difference of 0.25 eV. Other cation isomers show ionization energies of 7.30−7.84 eV.

For the neutral $(SiC)_{11}$ GM candidate, the adiabatic optimization of the corresponding cation failed. However, we found a very similar neutral $(SiC)_{11}$ cluster with a relative energy just 0.10 eV above the GM candidate, for which an adiabatic ionization optimization could be achieved. With an ionization energy of 6.64 eV it also corresponds to the lowest-energy cation configuration for n = 11. By inspecting the bond lengths of the neutral and cationic $(SiC)_{11}$ structure, we find that none of them changes significantly (max of 0.07 Å/bond) during the adiabatic ionization, which is reflected in the comparatively low energy difference of 0.18 eV. Higher-lying cation isomers have energies 6.92−7.35 eV above the neutral GM.

The GM candidate of neutral $(SiC)_{12}$ is found to be a bucky-like, spherical structure with strictly alternating Si-C bonds. However, our calculations for vertical and adiabatic ionization energies did not converge. The ionization of fullerene-shaped clusters is a dynamic and complex problem and requires high-level calculations and analyses (Hrodmarsson et al., 2020). For example, Buckminster fullerenes cations ($C_{60}{}^+$) undergo dynamic and pseudo Jahn-Teller effects lowering the icosahedral symmetry upon (photo-)ionization. Owing to these challenges, that are beyond the scope of this paper, we omit an in-depth investigation of the ionization of the "bucky" $(SiC)_{12}$ GM candidate isomer. Therefore, we calculate the ionization energies of an atom-segregated symmetric "butterfly"-shaped isomer, which is the second lowest-energy $(SiC)_{12}$ isomer according to our searches and has a relative energy of 0.54 eV. We find an ionization energy of 7.77 eV and that its geometry is hardly affected by the ionization process (max 0.02 Å/bond), which also explains the low energy difference (0.10 eV) between vertical and adiabatic ionization. We investigated two other isomers that result in ionization energies of 7.75 eV and 7.77 eV above the neutral GM.

4. SUMMARY AND CONCLUSIONS

The vertical and adiabatic single ionization energies of $(SiC)_n$, n = 1−12, span over a range of 6.59−10.64 eV and have an overall decreasing trend with cluster size *n*. In an astrophysical context, this energy range sets constraints for neutral $(SiC)_n$, n = 1−12, clusters to exist and therefore confines the conditions (temperature, radiation field) under which SiC nucleation can occur. The adiabatically optimized cation geometries indicate that the ionization predominantly takes place in the silicon-segregated part of t/he clusters. For n = 2,3,4 the lowest-energy cation does not correspond to the structural analog of the neutral GM candidate structures, but to a different geometry. For these sizes, the structural analog cations of the neutral GM show potential energies 0.83–1.66 eV and are hence metastable with respect to lowest-energy cation. Moreover, the optimization of the neutral GM structural analogs for sizes n = 3,4,5 leads to transition states (TSs) that are subsequently re-optimized and real minima are found.

Applying the kinetic gas theory to the presented range of ionization energies (6.59−10.64 eV) results in equivalent temperatures of ∼76,500−123,500 K. These temperatures are significantly higher than the characteristic temperatures in envelopes and winds of evolved stars, even when including non-equilibrium effects like shocks or other non-thermal heating processes. However, considering photo-ionization instead of ionization by a high temperature gas,the situation is different. For planetary nebulae with effective temperatures of ∼30,000 K, the radiation field peaks for photon energies in the range 6–10 eV (Cami et al., 2010). This photon energy range is almost superimposable with the range of (SiC)$_n$ ionization energies derived in this study. Therefore, we conclude that the ionization of (SiC)$_n$ clusters in low-mass AGB stars is viable, in particular toward the end of their lives, and that photo-ionization is most likely its responsible process.

DATA AVAILABILITY STATEMENT

The original contributions generated for the study are included in the article/supplementary material, further inquiries can be directed to the corresponding author/s.

AUTHOR CONTRIBUTIONS

DG conceived of the presented idea, performed the computations, discussed the results, and contributed to the final manuscript.

FUNDING

We acknowledge support from the ERC Consolidator Grant AEROSOL - Astrochemistry of Old Stars: direct probing of unique chemical laboratories 2016-2020 (PI Leen Decin), Project number 646758.

ACKNOWLEDGMENTS

We acknowledge the CINECA award under the ISCRA initiative, for the availability of high performance computing resources and support.

REFERENCES

Agúndez, M., Cernicharo, J., and Guélin, M. (2010). Photochemistry in the inner layers of clumpy circumstellar envelops: formation of water in C-rich objects and of C-bearing molecules in O-rich objects. *Astrophys. J.* 724, L133–L136. doi: 10.1088/2041-8205/724/2/L133

Amari, S., Lewis, R. S., and Anders, E. (1994). Interstellar grains in meteorites. I - Isolation of SiC, graphite, and diamond; size distributions of SiC and graphite. II - SiC and its noble gases. *Geochim. Cosmochim. Acta* 58:459. doi: 10.1016/0016-7037(94)90477-4

Belau, L., Wilson, K., Leone, S., and Ahmed, M. (2007). Vacuum ultraviolet (vuv) photoionization of small water clusters. *J. Phys. Chem. A* 111, 10075–10083. doi: 10.1021/jp075263v

Bernatowicz, T., Fraundorf, G., Ming, T., Anders, E., Wopenka, B., Zinner, E., et al. (1987). Evidence for interstellar SiC in the Murray carbonaceous meteorite. *Nature* 330, 728–730. doi: 10.1038/330728a0

Boldyrev, A. I., Simons, J., Zakrzewski, V. G., and von Niessen, W. (1994). Vertical and adiabatic ionization energies and electron affinities of new silicon-carbon (Si_nC) and silicon-oxygen (Si_nO) (n = 1-3) molecules. *J. Phys. Chem.* 98, 1427–1435. doi: 10.1021/j100056a010

Briant, M., Poisson, L., Hochlaf, M., de Pujo, P., Gaveau, M.-A., and Soep, B. (2012). Ar_2 photoelectron spectroscopy mediated by autoionizing states. *Phys. Rev. Lett.* 109:193401. doi: 10.1103/PhysRevLett.109.193401

Byrd, J. N., Lutz, J. J., Jin, Y., Ranasinghe, D. S., Montgomery, J. A., Perera, A., et al. (2016). Predictive coupled-cluster isomer orderings for some Si_mC_n (m, n < 12) clusters: a pragmatic comparison between DFT and complete basis limit coupled-cluster benchmarks. *J. Chem. Phys.* 145:024312. doi: 10.1063/1.4955196

Cami, J., Bernard-Salas, J., Peeters, E., and Malek, S. E. (2010). Detection of C_{60} and C_{70} in a young planetary Nebula. *Science* 329, 1180–1182. doi: 10.1126/science.1192035

Cernicharo, J., Gottlieb, C. A., Guelin, M., Thaddeus, P., and Vrtilek, J. M. (1989). Astonomical and laboratory detection of the SiC radical. *ApJ Lett.* 341, L25–L28. doi: 10.1086/185449

Cristallo, S., Nanni, A., Cescutti, G., Minchev, I., Liu, N., Vescovi, D., et al. (2020). Mass and metallicity distribution of parent AGB stars of presolar SiC. *Astron. Astrophys.* 644:A8. doi: 10.1051/0004-6361/202039492

Derbali, I., Hrodmarsson, H. R., Schwell, M., Benilan, Y., Poisson, L., Hochlaf, M., et al. (2020). Unimolecular decomposition of methyl ketene and its dimer in the gas phase: theory and experiment. *Phys. Chem. Chem. Phys.* 22, 20394–20408. doi: 10.1039/D0CP03921G

Drowart, J., De Maria, G., and Inghram, M. G. (1958). Thermodynamic study of sic utilizing a mass spectrometer. *J. Chem. Phys.* 29, 1015–1021. doi: 10.1063/1.1744646

Duan, X. F., Burggraf, L. W., and Huang, L. (2013). Searching for stable Si_nC_n clusters: combination of stochastic potential surface search and pseudopotential plane-wave car-parinello simulated annealing simulations. *Molecules* 18:8591. doi: 10.3390/molecules18078591

Friedemann, C. (1968). Siliziumkarbid als moglicher Bestandteil des interstellaren Staubes. *Astronomische Nachrichten* 291, 177–186. doi: 10.1002/asna.19682910405

Frisch, M. J., Trucks, G. W., Schlegel, H. B., Scuseria, G. E., Robb, M. A., Cheeseman, J. R., et al. *Gaussian 09, Revision E.01*. Wallingford, CT: Gaussian, Inc. (2009).

Gobrecht, D., Cherchneff, I., Sarangi, A., Plane, J. M. C., and Bromley, S. T. (2016). Dust formation in the oxygen-rich AGB star IK Tauri. *Astron. Astrophys.* 585:A6. doi: 10.1051/0004-6361/201425363

Gobrecht, D., Cristallo, S., Piersanti, L., and Bromley, S. T. (2017). Nucleation of small silicon carbide dust clusters in AGB stars. *Astrophys. J.* 840:117. doi: 10.3847/1538-4357/aa6db0

Guan, J., Hu, Y., Zou, H., Cao, L., Liu, F., Shan, X., et al. (2012). Competitive fragmentation pathways of acetic acid dimer explored by synchrotron VUV photoionization mass spectrometry and electronic structure calculations. *J. Chem. Phys.* 137:124308. doi: 10.1063/1.4754273

Hackwell, J. A. (1972). Long wavelength spectrometry and photometry of M, S and C-stars. *Astron. Astrophys.* 21:239.

Hoppe, P., Strebel, R., Eberhardt, P., Amari, S., and Lewis, R. S. (1996). Small SiC grains and a nitride grain of circumstellar origin from the Murchison meteorite: implications for stellar evolution and nucleosynthesis. *Geochim. Cosmochim. Acta* 60, 883–907. doi: 10.1016/0016-7037(95)00435-1

Hou, J., and Song, B. (2008). Density-functional study of structural and electronic properties of $Si_nC_n(n = 1\text{-}10)$ clusters. *J. Chem. Phys.* 128:154304. doi: 10.1063/1.2895051

Hrodmarsson, H. R., Garcia, G. A., Linnartz, H., and Nahon, L. (2020). VUV photoionization dynamics of the C60 buckminsterfullerene: 2D-matrix photoelectron spectroscopy in an astrophysical context. *Phys. Chem. Chem. Phys.* 22, 13880–13892. doi: 10.1039/D0CP01210F

Liu, N., Savina, M. R., Davis, A. M., Gallino, R., Straniero, O., Gyngard, F., et al. (2014). Barium isotopic composition of mainstream silicon carbides from murchison: constraints for s-process nucleosynthesis in asymptotic giant branch stars. *Astrophys. J.* 786:66. doi: 10.1088/0004-637X/786/1/66

Luo, Y. (2007). *Comprehensive Handbook of Chemical Bond Energies*. Boca Raton, FL: CRC Press. doi: 10.1201/9781420007282

Mahjoub, A., Hochlaf, M., Poisson, L., Nieuwjaer, N., Lecomte, F., Schermann, J.-P., et al. (2011). Slow photoelectron spectroscopy of d-valerolactam and its dimer. *ChemPhysChem* 12, 1822–1832. doi: 10.1002/cphc.201100090

Massalkhi, S., Agúndez, M., Cernicharo, J., Velilla Prieto, L., Goicoechea, J. R., Quintana-Lacaci, G., et al. (2018). Abundance of SiC_2 in carbon star envelopes - Evidence that SiC_2 is a gas-phase precursor of SiC dust. *Astron. Astrophys.* 611:A29. doi: 10.1051/0004-6361/201732038

McCarthy, M. C., Baraban, J. H., Changala, P. B., Stanton, J. F., Martin-Drumel, M.-A., Thorwirth, S., et al. (2015). Discovery of a missing link: detection and structure of the elusive disilicon carbide cluster. *J. Phys. Chem. Lett*. 6, 2107–2111. doi: 10.1021/acs.jpclett.5b00770

Peverati, R., and Truhlar, D. G. (2012). M11-l: a local density functional that provides improved accuracy for electronic structure calculations in chemistry and physics. *J. Phys. Chem. Lett*. 3, 117–124. doi: 10.1021/jz201525m

Thaddeus, P., Cummins, S. E., and Linke, R. A. (1984). Identification of the SiCC radical toward IRC +10216 - The first molecular ring in an astronomical source. *ApJ Lett*. 283, L45–L48. doi: 10.1086/184330

Treffers, R., and Cohen, M. (1974). High-resolution spectra of cool stars in the 10- and 20-micron regions. *Astrophys. J.* 188, 545–552. doi: 10.1086/152746

Zinner, E., Amari, S., Guinness, R., Jennings, C., Mertz, A., Nguyen, A., et al. (2007). NanoSIMS isotopic analysis of small presolar grains: search for Si_3N_4 grains from AGB stars and Al and Ti isotopic compositions of rare presolar SiC grains. *Geochim. Cosmochim. Acta* 71, 4786–4813. doi: 10.1016/j.gca.2007.07.012

Conflict of Interest: The author declares that the research was conducted in the absence of any commercial or financial relationships that could be construed as a potential conflict of interest.